Ain Shams Engineering Journal (2014) 5, 1199–1206

Ain Shams University

Ain Shams Engineering Journal

www.elsevier.com/locate/asej
www.sciencedirect.com

MECHANICAL ENGINEERING

Non-similar solutions for unsteady flow over a yawed cylinder with non-uniform mass transfer through a slot

G. Revathi [a], P. Saikrishnan [a], Ali Chamkha [b,*]

[a] Department of Mathematics, National Institute of Technology, Tiruchirappalli 620 015, Tamil Nadu, India
[b] Manufacturing Engineering Department, The Public Authority for Applied Education and Training, Shuweikh 70654, Kuwait

Received 4 December 2013; revised 26 March 2014; accepted 12 April 2014
Available online 23 May 2014

KEYWORDS

Unsteady flow;
Yawed cylinder;
Non-similar solution;
Forced convection flow;
Heat and mass transfer;
Control surfaces

Abstract Non-similar solutions are found numerically to a system of coupled non-linear partial differential equations indicating, unsteady laminar water boundary layer flow over yawed cylinder using implicit finite difference scheme along with Quasi-linearization technique. The fluid properties such as viscosity and Prandtl number are considered as an inverse function of temperature. Unsteadiness is caused by upstream velocity in and directions and non-uniform mass transfer (suction/injection) which is applied through slot on the surface of the geometry. The effect of yaw angle, variable fluid properties and non-uniform mass transfer on skin friction and heat transfer coefficients is analyzed. It is found that non-uniform slot suction and downstream movement of the slot cause the point of vanishing skin friction moves downstream, but non-uniform slot injection produces the opposite result of that corresponding to the suction case. When the yaw angle increases, both the skin friction coefficient in the – direction and the heat transfer coefficient decrease but the skin friction coefficient in the – direction increases for all times. The effect of the yaw angle is very little on the point of vanishing skin friction.

1. Introduction

Flow past yawed or unyawed bluff bodies are extensively encountered in engineering applications, such as cable suspension bridges, overhead cables, tow cables, chimney stacks, towers, offshore structures, subsea pipelines, and risers. Studying complex flow phenomena around a yawed cylindrical cable and reducing drag force and suppressing fluctuations in lift force are vital problems in engineering design. A number of investigators discussed the flow past a yawed cylinder by experimentally given in [1–3] and by numerically shown in [4]. Experimental results described that the force coefficients which are normalized by the velocity component perpendicular to the cylinder, are about independent on the yaw angle. This is often called the independence principle or the cosine law in the literature.

A detailed study of the literature about laminar flow past a yawed infinite circular cylinder with the assumption of

* Corresponding author. Tel.: +96566647697.
E-mail address: achamkha@yahoo.com (A. Chamkha).
Peer review under responsibility of Ain Shams University.

Production and hosting by Elsevier

2090-4479 © 2014 Production and hosting by Elsevier B.V. on behalf of Ain Shams University.
http://dx.doi.org/10.1016/j.asej.2014.04.009

constant fluid properties is given in [5–7]. In the work of Vasantha and Nath [5], self-similar solutions have been obtained for an unsteady compressible three-dimensional stagnation point boundary layer flow. For practical problems with temperature difference between the surface and the ambient fluid, the fluid properties such as viscosity and Prandtl number change undoubtedly and this influences the variation in velocity and thermal fields in the fluid flow. Under circumstances where large or moderate temperature gradients exist across the fluid medium, the assumption of constant fluid properties could cause significant errors. For example, the viscosity of water decreases by about and Prandtl number of water decreases by about respectively, when the temperature increases from $10\,^{\circ}\mathrm{C}(\mu = 1.307(\mathrm{g}\,10^{-2}\,\mathrm{cm}^{-1}\,\mathrm{s}^{-1}),\ \mathrm{Pr} = 9.45)$ to $50\,^{\circ}\mathrm{C}(\mu = 0.547(\mathrm{g}\,10^{-2}\,\mathrm{cm}^{-1}\,\mathrm{s}^{-1}),\ \mathrm{Pr} = 3.55)$ (see Table 1). In the recent studies on laminar water boundary layer flow with variable fluid properties over bluff bodies are given in [8–10]. In the work of Pop et al. [8], the viscosity of the fluid is assumed to vary with temperature and it is demonstrated that the assumption of constant properties may introduce severe errors in the prediction of surface friction factor and heat transfer rate. Non-similar solutions of unsteady flows have become important in current years in different categories of fluid mechanics and area of convective heat and mass transfer. The procedure of non-similarity solution methods for steady flows along with citations of relevant publications until 1967 is given by Deway and Gross [11]. Non-similar solutions for steady laminar boundary-layer flow over yawed cylinder with variable physical properties including heat and mass transfer have been obtained for compressible fluid by Roy [10] and for incompressible fluid by Roy and Saikrishnan [12]. But in unsteady flows the inclusion of time variable creates complexity in obtaining non-similar solutions from the starting point of the stream-wise co-ordinate to the point where skin friction vanishes. In the present analysis the upstream velocity in x and z directions is time dependent and cause unsteadiness in the flow. There is very less number of investigations in literature for non-similar solution technique to solve unsteady boundary layer flow problems compare to self-similar [5] and similarity solution techniques [13]. In the work of Takhar and Nath [13], an unsteady laminar incompressible boundary layer flow of an electrically-conducting fluid in the stagnation region of two-dimensional and axisymmetric bodies with an applied magnetic field is considered. It is found that the skin friction is strongly dependent on the magnetic parameter but, the heat transfer is weakly dependent on it, and also both skin friction and heat transfer are strongly dependent on the mass transfer parameter. Roy et al. [14] reported a non-similar solution an unsteady mixed convection flow over a vertical cone. So, as a step toward the development of non-similar solution technique to solve unsteady boundary layer flow problems, the boundary layer flow over yawed cylinder is considered for the current investigation, which have practical applications in Engineering. Excellent reviews of unsteady flows have been given in [15–18].

Mass transfer through a wall slot (i.e. mass transfer occurs in a small porous section of the body surface while there is no mass transfer in the remaining part of the body surface) into the boundary layer strongly influences the growth of a boundary layer along a surface and in particular can prevent or at least delay separation of the viscous region. It is of interest for various prospective applications together with thermal protections, energizing the inner portion of the boundary layer in adverse pressure gradient and skin friction reduction on control surfaces. The effect of slot injection (suction) into laminar compressible boundary layer over a flat plate by taking the interaction between the boundary layer and oncoming stream have been studied by researchers in Smith and Stewartson [19], Napolitano and Messick [20], Riley [21]. Despite uniform mass transfer, finite discontinuities arise at the leading and trailing edges of the slot and those can be avoided by choosing a non-uniform mass transfer distribution along a stream-wise slot and it has been discussed by Minkowycz et al. in [22] where, an investigation is made for a mixed convection flow on a vertical plate, that is either non-uniformly heated or cooled. Recently, different studies are reported the influence of non-uniform mass transfer on steady boundary layer flows over different geometries given in [23,12,24,25]. In the recent times the role of non-uniform mass transfer through double slot on the surface of the yawed cylinder in the steady boundary layer flow has been investigated by Saikrishnan in [26].

The wide literature on non-similar solution and mass transfer technique shows that the studies confined only for steady water boundary layer flow with non-uniform mass transfer. In the present analysis, an unsteady laminar water boundary layer flow over a yawed cylinder is considered. The simultaneous effect of non-uniform slot suction (injection) and yaw angle is studied on unsteady water boundary layer flow over yawed cylinder. The fluid considered, here, is water as it is one of the most common working fluids found in engineering applications. Flow around ocean structures and flow in industrial heat exchangers are two typical examples of such flows. The accurate prediction of water boundary layer flow field over a yawed infinite circular cylinder may be useful for undersea applications in the design of leading edge of many submerged bodies. In particular, the yawed infinite cylinder simulates approximately the leading edge of a swept-back wing of a body of high fineness ratio at an angle of attack and also allows a basic simplification of the complicated three-dimensional boundary layer equations. Thus, a detailed analysis of

Table 1 Values of thermo-physical properties of water at different temperature [28].

Temperature (T °C)	Density (ρ) (g cm^{-3})	Specific heat (C_p) (J 10^7 kg^{-1} K^{-1})	Thermal conductivity (k) (erg 10^5 cm^{-1} s^{-1} K^{-1})	Viscosity (μ) (g 10^{-2} cm^{-1} s^{-1})	Prandtl number (Pr)
0	1.0028	4.2176	0.561	1.793	13.48
10	0.9997	4.1921	0.58	1.307	9.45
20	0.99821	4.1818	0.5984	1.006	7.03
30	0.99565	4.1784	0.6154	0.7977	5.12
40	0.99222	4.1785	0.6305	0.6532	4.32
50	0.98803	4.1806	0.6435	0.547	3.55

the water boundary layer flow over a yawed cylinder taking non-similarity into account is of practical interest where the non-similarity may be due to the time dependent free stream velocity or due to the surface mass transfer or due to the curvature of the body or due to all the effects. Also it will be useful in understanding many boundary layer problems of practical importance for undersea applications as would arise, for example, in cooling gas turbine blades, suppressing recirculating bubbles and controlling transition and separation of the boundary layer over submerged bodies. In the present study non-similar solutions have been obtained for unsteady water boundary layer flows, starting from the origin of the streamwise co-ordinate to the point of vanishing skin friction. The values of skin friction and heat transfer rate have been obtained which are useful in determining the surface heat requirements for stabilizing the laminar boundary layer flow over a yawed cylinder in water.

2. Mathematical formulation

Consider an unsteady laminar non-similar water boundary-layer flow with temperature-dependent viscosity and Prandtl number over a yawed cylinder (see Fig. 1). Let us consider an orthogonal curvilinear coordinate system in which x-coordinate is the distance along the cylinder surface measured in the chordwise direction from the leading edge of the stagnation line and y is the coordinate normal to the cylinder surface and z is the spanwise coordinate. u, v and w are velocity components in x, y and z directions respectively. 'θ' is the yaw angle. Let the stream velocity (x and z direction) and mass transfer (injection/suction) vary with the axial distance (x) along the surface and with the time (t). The temperature difference between the wall and the free stream is small ($0\ ^\circ\mathrm{C} < T < 40\ ^\circ\mathrm{C}$). In spite of the variation in the both density (ρ) and the specific heat (c_p) with temperature is by less than 1% in the above mentioned temperature range, they are taken as constants (see Table 1). It is considered that the injected fluid possesses the same physical properties as the boundary-layer fluid. The blowing rate of the fluid is assumed to be small and it does not affect the inviscid flow at the edge of the boundary layer. The viscosity and the Prandtl number are assumed to vary as an inverse function of temperature and is taken from [27] and the numerical data, utilized for these correlations, are taken from Ref. [28].

$$\mu = \frac{1}{(b_1 + b_2 T)}, \quad Pr = \frac{1}{c_1 + c_2 T} \tag{1}$$

where

$$b_1 = 53.41, \quad b_2 = 2.43, \quad c_1 = 0.068 \quad \text{and} \quad c_2 = 0.004 \tag{2}$$

The boundary layer equations governing the flow can be expressed as [29]

$$u_x + v_y = 0 \tag{3}$$

$$u_t + uu_x + vu_y = (u_e)_t + u_e(u_e)_x + \rho^{-1}(\mu u_y)_y \tag{4}$$

$$w_t + uw_x + vw_y = (w_e)_t + \rho^{-1}(\mu w_y)_y \tag{5}$$

$$T_t + uT_x + vT_y = \rho^{-1}[(\mu/Pr)T_y]_y + (\mu/\rho c_p)\left(u_y^2 + w_y^2\right) \tag{6}$$

The initial and boundary conditions are:

$$\begin{aligned}
&u(x,y,0) = u(x,y), \quad v(x,y,0) = v(x,y),\\
&w(x,y,0) = w(x,y), \quad T(x,y,0) = T(x,y)\\
&u(x,0,t) = 0, \quad v(x,0,t) = v_w(x), \quad w(x,0,t) = 0,\\
&T(x,0,t) = T_w = \text{constant}\\
&u(x,\infty,t) = u_e(x,t), \quad w(x,\infty,t) = w_e(x,t),\\
&T(x,\infty,t) = T_\infty = \text{constant}.
\end{aligned} \tag{7}$$

R is radius of the cylinder, μ is dynamic viscosity, Pr is Prandtl number, $u_e(x,t)$ is the potential flow velocity at the edge of the boundary layer, $w_e(x,t)$ is the velocity at the edge of the boundary layer in $z-$direction and $v_w(x)$ denotes the surface mass transfer distribution. The coupled dimensional non-linear partial differential equations from (4)–(6) are made dimensionless using the following non-similarity transformation,

$$\xi = \int_0^x \left(\frac{U}{u_\infty}\right) d\left(\frac{x}{R}\right), \quad \eta = \left(\frac{Re}{2\xi}\right)^{1/2} \left(\frac{U}{u_\infty}\right)\left(\frac{y}{R}\right)$$

$$\psi(x,y,t) = u_\infty R \left(\frac{2\xi}{Re_1}\right)^{1/2} \phi(t^*) f(\xi,\eta,t^*)$$

$$G = \frac{T - T_\infty}{T_w - T_\infty}, \quad u = \frac{\partial \psi}{\partial y}, \quad v = -\frac{\partial \psi}{\partial x}, \quad w = w_e S$$

$$t^* = (3/2)Re_1(\mu_e/\rho R^2)t, \quad \phi(t^*) = 1 + 0.25t^{*2}, \quad t^* \geqslant 0$$

$$u_e(x,t) = U\phi(t^*), \quad u_\infty = U_\infty \cos\theta$$

The dimensionless governing equations are:

$$\begin{aligned}
&(NF_\eta)_\eta + \phi[fF_\eta + \beta(1 - F^2)] - P\left[F_{t^*} - \phi^{-1}\phi_{t^*}(1 - F)\right]\\
&= 2\xi\phi(FF_\xi - f_\xi F_\eta)
\end{aligned} \tag{8}$$

$$\begin{aligned}
&(NS_\eta)_\eta + \phi f S_\eta - P\left[S_{t^*} - (1 - S)\phi^{-1}\phi_{t^*}\right]\\
&= 2\xi\phi(FS_\xi - f_\xi S_\eta)
\end{aligned} \tag{9}$$

$$\begin{aligned}
&(NPr^{-1}G_\eta)_\eta + \phi f G_\eta + NEc\left[(U\phi/u_\infty)^2 \cos^2\theta F_\eta^2 + \phi^2 \sin^2\theta S_\eta^2\right]\\
&- PG_{t^*} = 2\xi\phi(FG_\xi - f_\xi G_\eta)
\end{aligned} \tag{10}$$

with boundary conditions

$$\begin{aligned}
&F(\xi,0,t) = 0, \quad S(\xi,0,t) = 0, \quad G(\xi,0,t) = 1 \quad \text{at} \quad \eta = 0\\
&F(\xi,\infty,t) = 1, \quad S(\xi,\infty,t) = 1, \quad G(\xi,\infty,t) = 0 \quad \text{at} \quad \eta = \eta_\infty
\end{aligned} \tag{11}$$

where

$$N = \mu/\mu_\infty = \frac{(b_1 + b_2 T_\infty)}{(b_1 + b_2 T)} = \frac{1}{(1 + a_1 G)}$$

$$Pr = \frac{1}{(c_1 + c_2 T)} = \frac{1}{(a_2 + a_3 G)}$$

$$a_1 = \frac{b_2 \Delta T_w}{(b_1 + b_2 T_\infty)}, \quad a_2 = c_1 + c_2 T_\infty, \quad a_3 = c_2 \Delta T_w,$$

$$\Delta T_w = (T_w - T_\infty), \quad u = u_e F, \quad w = w_e S, \quad Re = \frac{\rho u_\infty R}{\mu_\infty}$$

$$v = -\left(\frac{2}{Re_1}\right)^{1/2} u_\infty R\phi\left[\xi^{1/2}(f_\xi \xi_x + f_\eta \eta_x) + \frac{f}{2\sqrt{\xi}}\xi_x\right],$$

$$P = 3\xi(u_\infty/U)^2,$$

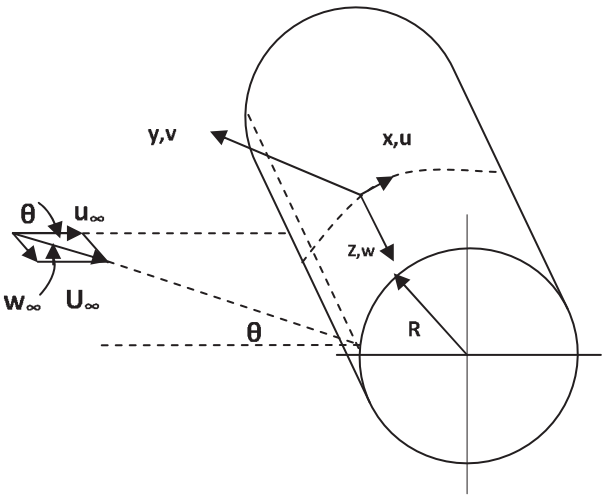

Fig. 1 Coordinate system and flow model.

$$\beta(\xi) = (2\xi/U)(dU/d\xi), \quad Ec = U_\infty^2/[c_p(\Delta T_w)]$$

$$f = \int_0^\eta F d\eta + f_w,$$

$$f_w = -(2P_1)^{-1/2}\phi^{-1}\left(\frac{Re}{2}\right)^{1/2}\int_0^{x/R}(v_w/u_\infty)d(x/R). \tag{12}$$

Here f_w is the stream function value at wall. In the present analysis, unsteadiness and non-similarity are both due to the external velocity at the edge of the boundary layer in x- and z-directions, $u_e(\bar{x},t)$, $w_e(\bar{x},t)$ respectively (where $\bar{x}$ is the dimensionless distance along the surface) and the normal component of the velocity at the surface, $v(\bar{x},t)$. The free-stream velocity distribution at the edge of the boundary layer for the case of two-dimensional flow over a circular cylinder can be expressed as,

$$u_e/u_\infty = 2\sin\bar{x}\phi(t^*), \quad U/u_\infty = 2\sin\bar{x}, \quad \bar{x} = x/R$$

$$w_e(x,t) = w_\infty\phi(t^*), \quad w_\infty = U_\infty\sin\theta \tag{13}$$

The expressions for ξ, β, f_w, P, C_f, $\overline{C}_f$, Nu are respectively given by,

$$\xi = 2Q_1, \quad \beta = \frac{2\cos\bar{x}}{Q_2}, \quad P = \frac{3}{2Q_2} \tag{14}$$

$$f_w = \begin{cases} 0, & \bar{x} \leqslant \bar{x}_0 \\ A\phi^{-1}(2Q_1)^{-1/2}C(\bar{x},\bar{x}_0), & \bar{x}_0 \leqslant \bar{x} \leqslant \bar{x}_0^*, \\ A\phi^{-1}(2Q_1)^{-1/2}C(\bar{x}_0^*,\bar{x}_0), & \bar{x} \geqslant \bar{x}_0^*, \end{cases} \tag{15}$$

where the function

$$C(\bar{x},\bar{x}_0) = 1 - \cos\{\omega^*(\bar{x}-\bar{x}_0)\}, \quad Q_1 = 1-\cos\bar{x},$$
$$Q_2 = 1+\cos\bar{x}.$$

here v_w is taken as,

$$v_w = \begin{cases} -u_\infty\left(\frac{Re_L}{2}\right)^{-1/2}A\omega^*\sin\{\omega^*(\bar{x}-\bar{x}_0)\}, & \bar{x}_0 \leqslant \bar{x} \leqslant \bar{x}_0^* \\ 0, & \bar{x} \leqslant \bar{x}_0 \text{ and } \bar{x} \geqslant \bar{x}_0^* \end{cases} \tag{16}$$

$$\xi\frac{\partial}{\partial\xi} = B(\bar{x})\frac{\partial}{\partial\bar{x}} \quad \text{where} \quad B(\bar{x}) = \tan\left(\frac{\bar{x}}{2}\right), \tag{17}$$

Using relation (17), (13) and (14) it is convenient to write Eqs. (8)–(10) in terms of $\bar{x}$ instead of ξ,

$$(NF_\eta)_\eta + \phi[fF_\eta + \beta(1-F^2)] - P[F_{t^*} - \phi^{-1}\phi_{t^*}(1-F)] = 2B(\bar{x})\phi(FF_{\bar{x}} - f_{\bar{x}}F_\eta) \tag{18}$$

$$(NS_\eta)_\eta + \phi f S_\eta - P[S_{t^*} - (1-S)\phi^{-1}\phi_{t^*}] = 2B(\bar{x})\phi(FS_{\bar{x}} - f_{\bar{x}}S_\eta) \tag{19}$$

$$(NPr^{-1}G_\eta)_\eta + \phi f G_\eta + NEc\left[(U\phi/u_\infty)^2\cos^2\theta F_\eta^2 + \phi^2\sin^2\theta S_\eta^2\right] - PG_{t^*} = 2B(\bar{x})\phi(FG_{\bar{x}} - f_{\bar{x}}G_\eta) \tag{20}$$

with boundary condition,

$$F(\bar{x},0,t) = 0, \quad S(\bar{x},0,t) = 0, \quad G(\bar{x},0,t) = 1 \quad \text{at} \quad \eta = 0$$
$$F(\bar{x},\infty,t) = 1, \quad S(\bar{x},\infty,t) = 1, \quad G(\bar{x},\infty,t) = 0$$
$$\text{at} \quad \eta = \eta_\infty \tag{21}$$

The skin friction coefficients in x- and z-direction and heat transfer coefficient can be expressed as,

$$C_f(Re)^{1/2} = 4\phi(\cos\theta)^{3/2}Q_2Q_1^{1/2}N_w(F_\eta)_w, \tag{22}$$

$$\overline{C}_f(Re)^{1/2} = 2^{3/2}\phi\sin\theta(\cos\theta)^{1/2}\cos\left(\frac{\bar{x}}{2}\right)N_w(S_\eta)_w, \tag{23}$$

$$Nu(Re)^{-1/2} = -2^{1/2}(\cos\theta)^{1/2}\cos\left(\frac{\bar{x}}{2}\right)(G_\eta)_w \tag{24}$$

where

$$C_f = \frac{2\left[\mu\frac{\partial u}{\partial y}\right]_w}{\rho U_\infty^2}, \quad \overline{C}_f = \frac{2\left[\mu\frac{\partial w}{\partial y}\right]_w}{\rho U_\infty^2}, \quad Nu = -\frac{R\left(\frac{\partial T}{\partial y}\right)_w}{T_w - T_\infty}.$$

3. Solution procedure

The set of non-linear coupled partial differential Eqs. (18)–(20) with boundary conditions (21) have been linearized using Quasilinearization technique [30]. This technique can be viewed as a generalization of Newton–Raphson approximation technique in functional space. Now the linear system of coupled partial differential equations is given below,

$$X_1^iF_{\eta\eta}^{i+1} + X_2^iF_\eta^{i+1} + X_3^iF^{i+1} + X_4^iF_{\bar{x}}^{i+1} + X_5^iG_\eta^{i+1} + X_6^iG^{i+1} + X_7^iF_{t^*}^{i+1} = X_8^i \tag{25}$$

$$Y_1^iS_{\eta\eta}^{i+1} + Y_2^iS_\eta^{i+1} + Y_3^iS^{i+1} + Y_4^iS_{\bar{x}}^{i+1} + Y_5^iG_\eta^{i+1} + Y_6^iG^{i+1} + Y_7^iF^{i+1} + Y_8^iS_{t^*}^{i+1} = Y_9^i \tag{26}$$

$$Z_1^iG_{\eta\eta}^{i+1} + Z_2^iG_\eta^{i+1} + Z_3^iG^{i+1} + Z_4^iG_{\bar{x}}^{i+1} + Z_5^iS_\eta^{i+1} + Z_6^iF_\eta^{i+1} + Z_7^iF^{i+1} + Z_8^iG_{t^*}^{i+1} = Z_9^i \tag{27}$$

With boundary condition,

$$F^{k+1} = 0 \quad S^{k+1} = 0 \quad G^{k+1} = 1 \quad \text{at} \quad \eta = 0$$
$$F^{k+1} = 1 \quad S^{k+1} = 1 \quad G^{k+1} = 0 \quad \text{at} \quad \eta = \eta_\infty \tag{28}$$

Where η_∞ is the edge of the boundary layer. The coefficient functions with iterative index i are known where the functions with iterative index $(i+1)$ are to be determined. The above resultant system of iterative linear partial differential Eqs.

(25)–(27) has been discritized by implicit finite difference method given in [12]. The difficulties arise at the starting point of the streamwise coordinate and at the point of vanishing skin friction are overcome by applying the implicit finite difference scheme along with the Quasilinearization technique and an appropriate selection of finer step sizes in the streamwise direction. The unique feature of Quasi-linear implicit finite difference scheme as quadratic convergence and monotonicity has been found superior than the built-in iteration of upwind technique or finite amplitude technique. The efficiency and accuracy of the method have been illustrated through it's applications to many boundary value problems in the book by Bellman and Kalaba [30]. Finally, the obtained system of algebraic equations forms a block tri-diagonal matrix and which have been solved by Varga algorithm [31]. The grid sizes $\Delta\eta$, $\Delta\bar{x}$, Δt^* have been optimized and taken as $\Delta\eta = 0.02$, $\Delta t^* = 0.1$ throughout the computation. In the $\bar{x}$-direction, $\Delta\bar{x} = 0.01$ has been used for small values of $\bar{x}(\bar{x} \leqslant 0.45)$, then it has been decreased to $\Delta\bar{x} = 0.005$. This value of $\Delta\bar{x}$ has been used for $\bar{x} \leqslant 1.15$, thereafter the step size has been reduced further, ultimately choosing a value $\Delta\bar{x} = 0.0001$ in the neighborhood of the point of vanishing skin friction, to ensure the convergence of the numerical solution to the exact solution. The grid sizes have been optimized because the convergence becomes slower when the point of vanishing skin friction in the chord-wise direction is approached. Further reduction in grid sizes will not affect the result up to the fourth decimal places. The value of η_∞ (i.e. the edge of the boundary layer) has been taken as 6.0. A convergence criteria based on the relative difference between the current and previous iteration values are employed. When the difference reaches less than 10^{-4}, the solution is assumed to have converged and the iterative process is terminated. (i.e.)

$$Max\left\{\left|(F_\eta)_w^{k+1} - (F_\eta)_w^k\right|, \quad \left|(S_\eta)_w^{k+1} - (S_\eta)_w^k\right|, \times \left|(G_\eta)_w^{k+1} - (G_\eta)_w^k\right|\right\} < 10^{-4}.$$

4. Results and discussion

Computations have been carried out for various values of time t^* $(0 \leqslant t^* \leqslant 2)$, yawed angle $\theta(0° \leqslant \theta \leqslant 45°)$ and mass transfer parameter $A(-0.1 \leqslant A \leqslant 0.25)$ on a Intel(R)core(TM)i5 CPU digital computer system. One sample calculation (for $t^* = 2$, $\theta = 30°$, $A = 0.25$) takes approximately 20 min CPU time and the memory used to store the results is 585 KB on the above mentioned computer system. In all numerical computations the fluid properties such as viscosity and Prandtl number are taken as an inverse function of temperature. In order to verify the correctness of the procedure, the skin friction and heat transfer coefficients have been obtained for time $t^* = 0$ for different mass transfer values ($A = -0.1, 0, 0.25$) and those values are compared with the solutions given by Roy and Saikrishnan [12]. Also the values of skin friction rate and velocity profile have been compared with the already existing results of Eswara and Nath [9] for a particular case by assuming $A = 0$, $\theta = 0°$, $T_\infty = 18.7$, $\Delta T_w = 10.0$. The results are found in an excellent agreement and the comparisons are shown in Fig. 2.

Fig. 3 represents the velocity (x, z directions) and temperature profiles of the fluid flow at different times $t^* = 0$ and $t^* = 2$. It is observed that the velocity and temperature boundary layer thickness decrease with suction, while injection has opposite effect. The reason is that the low energy fluid particles in the boundary layer are removed by suction which causes the thickness of both velocity and temperature boundary layers to

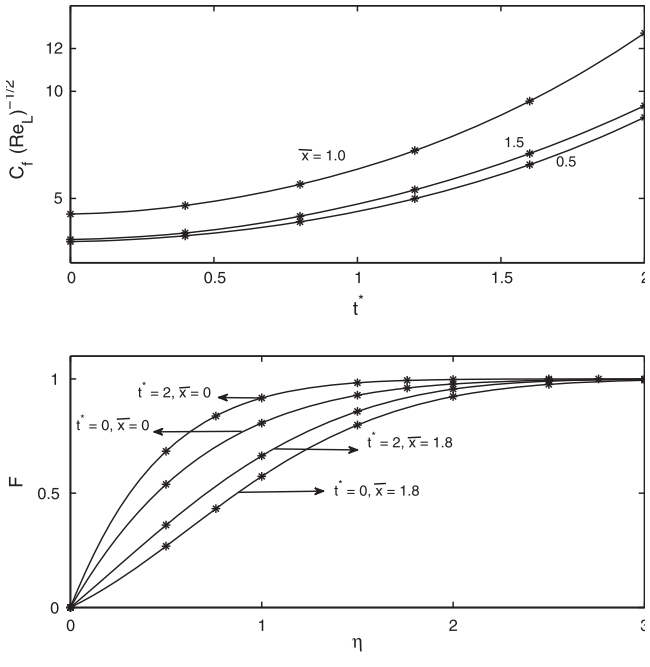

Fig. 2 Comparison of skin friction and velocity profile with particular case of flow over cylinder for $Ec = 0$, $\theta = 0°$, $A = 0$, $T_w = 18.7$ °C, $\Delta T_w = 10.0$ °C, $\varphi(t^*) = 1 + \varepsilon t^{*2}$, $\varepsilon = 0.25$. _____ present results, * Eswara and Nath [9].

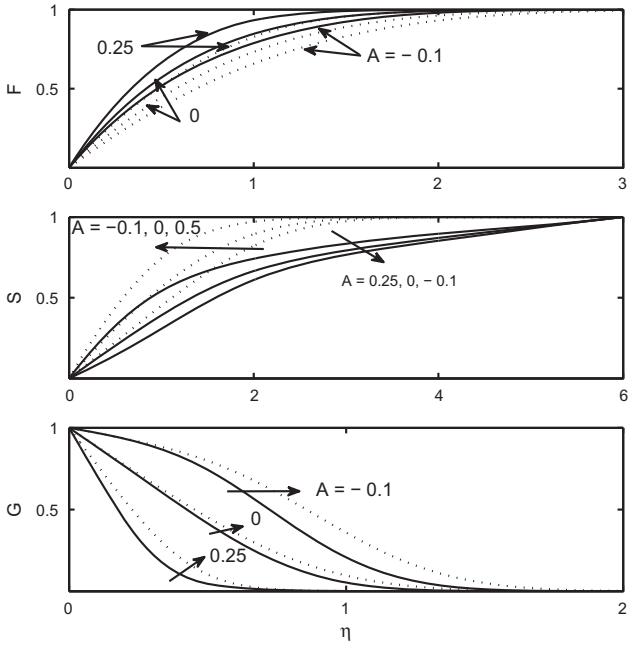

Fig. 3 Effect of non-uniform mass transfer (A) on velocity profiles (x, z directions) and temperature profile for different times $t^* = 0$ (---------) and $t^* = 2$ (——) at the point $\bar{x} = 1.4$ with $\varphi(t^*) = 1 + \varepsilon t^{*2}$, $\varepsilon = 0.25$, $Ec = 0$, $\theta = 30°$, $T_w = 18.7$ °C, $\Delta T_w = 10.0$ °C, $\omega^* = 2\pi$. Slot $\left[\overline{x_0} = 0.8 - \overline{x_0^*} = 1.3\right]$.

decrease. Also it is found that, unsteadiness decreases the thickness of both velocity (x-direction) and temperature boundary layer but, increases the thickness of velocity (z-direction) boundary layer. The reason is that, as time increases, there is an enhancement of velocity ($u_e = U\phi(t^*)$) and thus there is a decrease in the momentum boundary layer. Similarly, the effect of increasing values of the unsteadiness is to decrease the temperature field and hence, the thermal boundary layer thickness decreases. Since the flow dominates in the span-wise direction, the boundary layer thickness increases in the span-wise direction for increasing times.

Fig. 4 displays the effect of mass transfer $A(-0.1 \leqslant A \leqslant 0.25)$ on skin friction (x and z directions) and heat transfer coefficients over the time interval $[0,2]$. It is observed from the figure that, for all time t^*, both skin friction (x and z directions) and heat transfer coefficients increase with suction ($A > 0$), but decrease with injection ($A < 0$). For the quantitative analysis, the values of $C_f(Re)^{1/2}$, $\overline{C_f}(Re)^{1/2}$ and $Nu(Re)^{-1/2}$ have been calculated at the point $\bar{x} = 1.6$, time $t^* = 1$ and for the yaw angle $\theta = 30°$ and those values are increasing approximately by 34.3%, 90.3% and 149.8% respectively, with the increase in suction from $A = 0$ *to* $A = 0.25$. While in the case of injection, the values of $C_f(Re)^{1/2}$, $\overline{C_f}(Re)^{1/2}$ and $Nu(Re)^{-1/2}$ have been calculated at the point $\bar{x} = 1.6$, time $t^* = 1$ and for the yaw angle $\theta = 30°$ and those values are decreasing approximately by 20.5%, 46.8% and 80.5% respectively, with the increase in injection from$A = 0$ to $A = -0.1$. The physical reason is that, when the fluid near the wall is being sucked through the slot, the fluid in the boundary layer comes closer to surface. Due to comparatively high energy particles coming closer to the surface, the velocity and temperature gradients increase in the slot. The opposite result occurs in the case of injection since the fluid is injected into boundary layer.

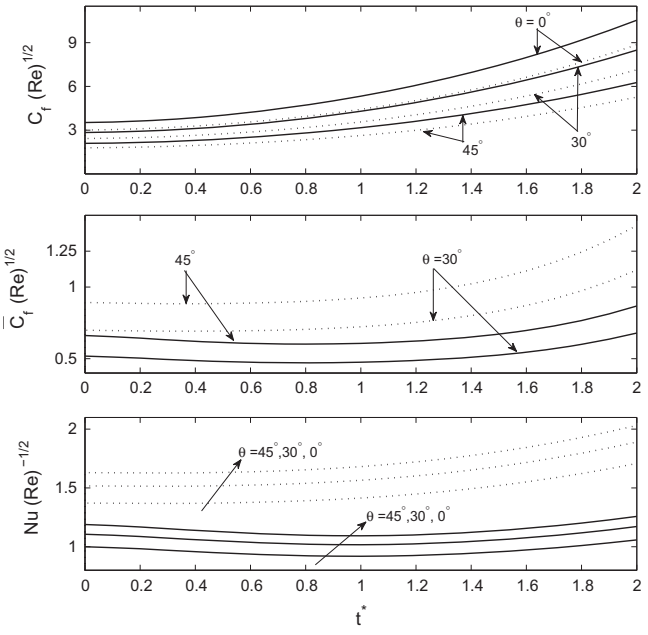

Fig. 5 Effects of time (t^*) and yaw angle (θ) on skin friction coefficients (directions) and heat transfer coefficient at different positions $\bar{x} = 0.5$ (-------) and$\bar{x} = 1.4$ (——) with $\varphi(t^*) = 1 + \varepsilon t^{*2}$, $\varepsilon = 0.25$, $Ec = 0$, $A = 0$, $T_w = 18.7$ °C, $\Delta T_w = 10.0$ °C.

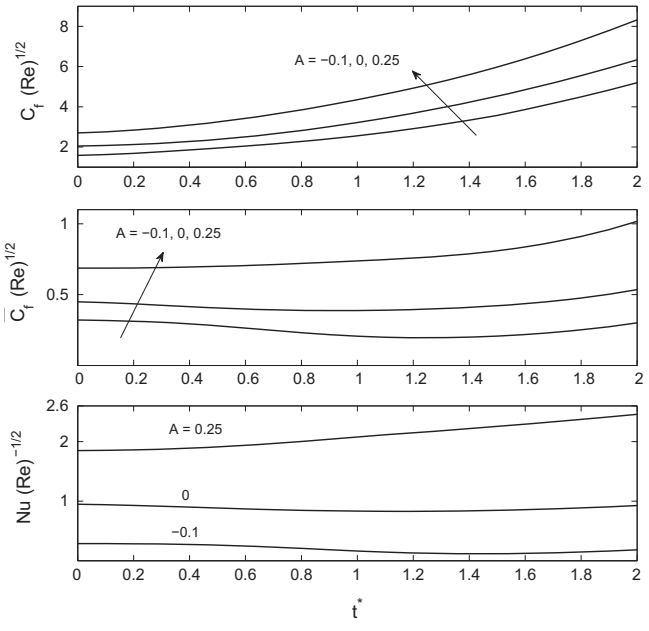

Fig. 4 Effects of time (t^*) and mass transfer (A) on skin friction coefficients (directions) and heat transfer coefficient at the point $\bar{x} = 1.6$ with $\varphi(t^*) = 1 + \varepsilon t^{*2}$, $\varepsilon = 0.25$, $Ec = 0$, $\theta = 30°$, $T_w = 18.7$ °C, $\Delta T_w = 10.0$ °C, $\omega^* = 2\pi$. Slot $\left[\overline{x_0} = 1.0 - \overline{x_0^*} = 1.5\right]$.

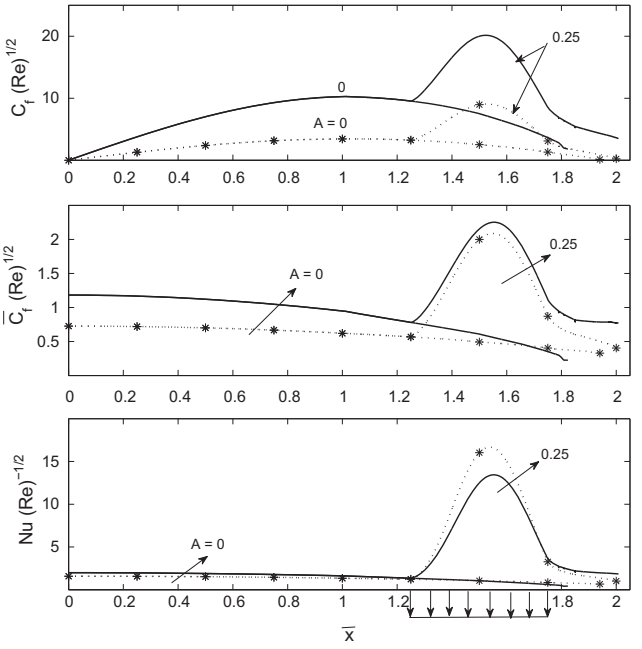

Fig. 6 Effect of suction ($A > 0$) on skin friction coefficients (directions) and heat transfer coefficient for different times $t^* = 0$ (----------) and $t^* = 2$ (——) with φ $(t^*) = 1 + \varepsilon t^{*2}$, $\varepsilon = 0.25$, $Ec = 0$, $\theta = 30°$, $T_w = 18.7$ °C, $\Delta T_w = 10.0$ °C, $\omega^* = 2\pi$. Slot $\left[\overline{x_0} = 1.25 - \overline{x_0^*} = 1.75\right]$.

Fig. 5 depicts the effect of yaw angle ($0° \leqslant \theta \leqslant 45°$) on skin friction ($x$, z directions) and heat transfer coefficients at different points $\bar{x} = 0.5, 1.4$ in the time interval t^* [0,2]. As the yaw angle (θ) increases from $\theta = 0°$ to $\theta = 45°$, for the time interval t^* [0,2], the skin friction coefficient in x-direction and heat transfer coefficient decrease whereas, skin friction coefficient in z-direction increases. The reason is that the flow dominates in the z-direction as θ increases, so that the values of $\overline{C_f}(Re)^{1/2}$ increases, whereas the values of $C_f\ (Re)^{1/2}$ and $Nu(Re)^{-1/2}$ decreases.

Figs. 6 and 7 demonstrate the effect of the suction and injection parameter on the skin friction (x and z directions) and heat transfer coefficients, respectively when the time $t \geqslant 0$ for the yaw angle $\theta = 30°$. In the case of non-uniform slot suction, the values of $C_f(Re)^{1/2}$, $\overline{C_f}(Re)^{1/2}$ and $Nu(Re)^{-1/2}$ increase in magnitude as the slot starts and attain their maximum values in the center of the slot and decrease from their maximum values toward the trailing edge of the slot for $t \geqslant 0$. For the fixed yaw angle θ, the skin friction increases in both the x, z directions as time increases due to loss in kinetic energy of fluid particles, whereas there is not much variation in the heat transfer coefficient. In particular, in the slot, the heat transfer coefficient decreases as time increases because of continuous suction of fluid from the boundary layer. From these figures, it is also observed that the non-uniform slot suction causes the location of zero skin friction to move downstream, because of the low energy fluid particles in the boundary layer is removed and behind the slot a new boundary layer forms which can overcome a certain pressure increase and hence, the reverse flow region moves downstream as suction increases. The effect of injection is just the opposite of the effect of suction.

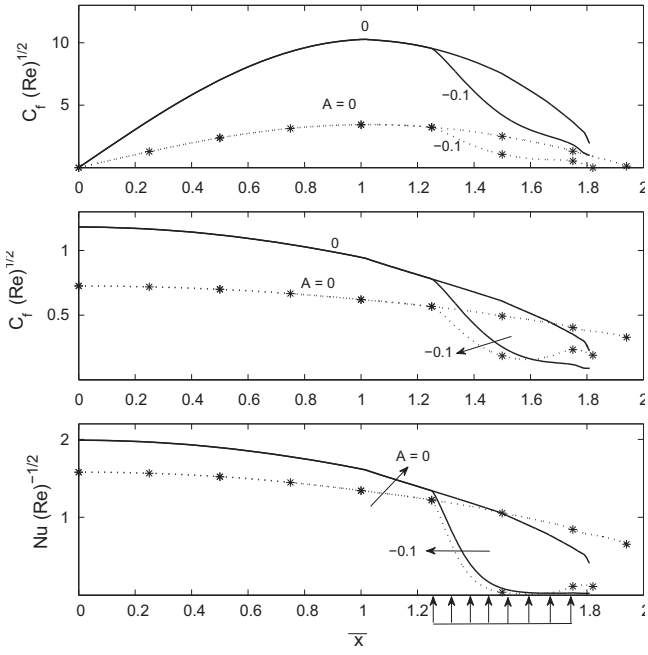

Fig. 7 Effect of injection ($A < 0$) on skinfriction coefficients (directions) and heat transfer coefficient for different times $t^* = 0$ (----------) and $t^* = 2$ (——) with $\varphi\ (t^*) = 1 + \varepsilon t^{*2}$, $\varepsilon = 0.25$, $Ec = 0$, $\theta = 30$ °C, $T_w = 18.7$ °C, $\Delta T_w = 10.0$ °C, $\omega^* = 2\pi$. Slot $\left[1.25 - \overline{x_0^*} = 1.75\right]$.

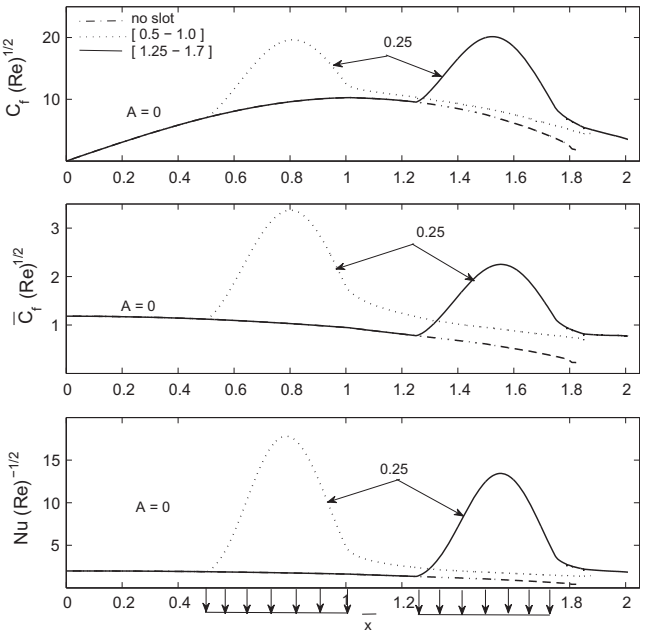

Fig. 8 Effect of slot location on skin friction coefficients (directions) and heat transfer coefficient at time $t^* = 2$ with $\varphi(t^*) = 1 + \varepsilon t^{*2}$, $\varepsilon = 0.25$, $Ec = 0$, $\theta = 30°$, $T_w = 18.7$ °C, $\Delta T_w = 10.0$ °C, $\omega^* = 2\pi$. Slot is placed at $\left[\overline{x_0} = 0.5 - \overline{x_0^*} = 1.0\right]$ and $\left[\overline{x_0} = 1.25 - \overline{x_0^*} = 1.75\right]$.

The effect of slot movement on skin friction (x, z directions) and heat transfer coefficients have been depicted in Fig. 8 at the time $t^* = 2$ and with the yaw angle $\theta = 30°$. It is observed that, if the slot is moved downstream, the adverse pressure gradient region also moves downstream. Thus the reverse flow region can be moved downstream by imposing the non-uniform slot suction and also by moving the slot downstream.

5. Conclusion

The non-similar solutions for an unsteady laminar incompressible water boundary layer flow over a yawed cylinder with temperature dependent fluid properties and non-uniform mass transfer through a slot have been obtained from the origin of the stream wise co-ordinate to the point of vanishing skin friction.

1. As suction increases both velocity and temperature boundary layer thickness decreases.
2. As time increases from zero to one, the velocity (x-direction) and temperature boundary layer thickness decrease but the velocity (z-direction) boundary layer thickness increases.
3. For the fixed yaw angle θ, the skin friction increases in both the x, z directions as time increases due to loss in kinetic energy of fluid particles, whereas there is not much variation in the heat transfer coefficient.
4. When the yaw angle increases, both skin friction coefficient in x-direction and heat transfer coefficient decrease but the skin friction coefficient in z-direction increase for all times.

5. Suction and the downstream movement of slot cause the point of vanishing skin friction moves downstream.
6. Injection has opposite effect of suction.

Acknowledgements

P. Saikrishnan would like to express thanks to Department of Science & Technology, New Delhi, India for the financial support for the research project (SR/FTP/MS-06/2009) under SERC Fast Track Scheme. The authors are also thankful to the reviewers for their comments which resulted in significant improvement in the quality of this article.

References

[1] King R. Vortex excited oscillations of yawed circular cylinders. ASME J Fluids Eng 1977;99:495–502.
[2] Ramberg S. The effects of yaw and finite length upon the vortex wakes of stationary and vibrating circular cylinders. J Fluid Mech 1983;128:81–107.
[3] Thakur A, Liu X, Marshall JS. Wake flow of single and multiple yawed cylinders. J Fluids Eng 2004;126:861–70.
[4] Marshall JS. Wake dynamics of a yawed cylinder. J Fluids Eng 2003;125:97–103.
[5] Vasantha R, Nath G. Self similar solutions of an unsteady compressible three-dimensional stagnation point boundary layer flow with massive blowing. Int J Eng Sci 1985;23:561.
[6] Chiu WS, Lienhard JH. On real fluid flow over yawed circular cylinders. J Basic Eng 1967;89(4):851.
[7] Cooke JC. The boundary-layer of a class of infinite yawed cylinder. Proc Cambridge Philos Soc 1950;46:645.
[8] Pop I, Gorla RSR, Rashidi M. The effect of variable viscosity on flow and heat transfer to a continuous moving flat plate. Int J Eng Sci 1992(30):1–6.
[9] Eswara AT, Nath G. Unsteady two-dimensional and axisymmetric water boundary layers with variable viscosity and Prandtl number. Int J Eng Sci 1994;32:267–79.
[10] Roy S. Non-uniform mass transfer or wall enthalpy into a compressible flow over yawed cylinder. Int J Heat Mass Transfer 2001;44:3017–24.
[11] Dewey CF, Gross JF. Exact solutions of the laminar boundary-layer equations. Adv Heat Transfer 1967;4(13):317.
[12] Roy S, Saikrishnan P. Non-unifrom slot injection (suction) into water boundary layer flow past yawed cylinder. Int J Eng Sci 2004;42:2147–57.
[13] Takhar HS, Nath G. Similarity solution of unsteady boundary layer equations with a magnetic field. Meccanica 1997;32:157–63.
[14] Roy S, Datta Prabal, Mahanti NC. Non-similar solution of an unsteady mixed convection flow over a vertical cone with suction or injection. Int J Heat Mass Transfer 2007;50:181–7.
[15] Riley N. Unsteady laminar boundary layers. SIAM Rev 1975;17:274–97.
[16] McCorosky WJ. Some current research in unsteady fluid dynamics. J Fluids Eng 1977;99:8–39.
[17] Telionis DP. Review-unsteady boundary layers separated and aattached. J Fluids Eng 1979;101:29–44.
[18] Telionis DP. Unsteady viscous flows. New York: Springer; 1981.
[19] Smith FT, Stewartson K. On slot injection into a supersonic laminar boundary layers. Proc Roy Soc Lond A 1973;332:1–22.
[20] Napolitano M, Messick RE. On strong slot injection into a subsonic laminar boundary layer. Comput Fluids 1980;8:199–212.
[21] Riley N. Non-uniform slot injection into a boundary layer. J Eng Math 1981;15:299–314.
[22] Minkowycz WJ, Sparrow EM, Schneider GE, Pletcher RH. Hand book of numerical heat transfer. New York: Wiley; 1988, p. 140–144.
[23] Saikrishnan P, Roy S. Non-Uniform slot injection (suction) into water boundary layers over (i) a cylinder and (ii) a sphere. Int J Eng Sci 2003;41:1351–65.
[24] Roy S, Saikrishnan P. Non-uniform slot injection (suction) into steady laminar water boundary layer flow over a rotating sphere. Int J Heat Mass Transfer 2003;46:3389–96.
[25] Ravindran R, Roy Satyajit, Momoniat E. Effects of injection (suction) on a steady mixed convection boundary layer flow over a vertical cone. Int J Numer Methods Heat Fluid Flow 2009;19(3/):432–44.
[26] Saikrishnan Ponnaiah. Boundary layer flow over a yawed cylinder with variable viscosity: role of non-uniform double slot suction (injection). Int J Numer Methods Heat Fluid Flow 2012;22(3):342–56.
[27] Schlichting H. Boundary layer theory. New York: Springer; 2000.
[28] Lide DR, editor. CRC hand book of chemistry and physics. Boca Raton, FL: CRC Press; 1990.
[29] Vasantha R, Nath G. Unsteady nonsimilar laminar incompressible boundary layer flow over a yawed infinite circular cylinder. J Appl Mech 1985;52(2):496–8.
[30] Bellman RE, Kalaba RE. Quasilinearization and non-linear boundary value problem. New York: American Elsevier Publishing Co. Inc.; 1965.
[31] Varga RS. Matrix iterative analysis. New York: Springer; 2000.